Carbohydrate Research 345 (2010) 2381–2389

Contents lists available at ScienceDirect

Carbohydrate Research

journal homepage: www.elsevier.com/locate/carres

Conformational fluctuation in palladium(II)–methyl aldopentopyranoside complexes

Thorsten Allscher, Yvonne Arendt, Peter Klüfers *

Department of Chemistry and Biochemistry, Ludwig-Maximilians-Universität, Butenandtstraße 5-13, D-81377 Munich, Germany

ARTICLE INFO

Article history:
Received 29 June 2010
Received in revised form 9 August 2010
Accepted 12 August 2010
Available online 24 August 2010

Keywords:
Methyl aldopentosides
Monosaccharide chelates
Palladium
Chair inversion

ABSTRACT

Four methyl D-pentopyranosides (β-Ara, α-Lyx, β-Rib, β-Xyl), as well as Me-β-L-Ara, some of them residing in a well-defined conformation in the solution state (Ara, Xyl) and some showing pronounced chair inversion in solution (Lyx, Rib), form bidentate chelates of the general formula [Pd(chxn)(LH_{-2})-κ*O*,*O*′] and [Pd(tmen)(LH_{-2})-κ*O*,*O*′], chxn = (*R*,*R*)-cyclohexane-1,2-diamine, tmen = *N*,*N*,*N*′,*N*′-ethane-1,2-diamine and L = glycoside, with $Pd^{II}N_2$-type metal probes. The dynamic behaviour of the free glycosides is maintained in their chelates, the only case where the metal is bonded by a cis-vicinal diol function. Thus, one fluctuating chelate was detected with the lyxopyranoside in the κ$O^{2,3}$ binding mode, and two fluctuating chelates were found for the ribopyranoside (κ$O^{2,3}$ and κ$O^{3,4}$). No fluctuating chelate was found for the arabinopyranoside (the free arabinopyranoside being non-fluctuating as well), or for the xylopyranoside (no cis-vicinal diol function). In addition, *syn*-diaxial chelation (κ$O^{2,4}$) was observed for the ribopyranoside and the xylopyranoside. The spectroscopic results were supplemented by X-ray analyses.

© 2010 Elsevier Ltd. All rights reserved.

1. Introduction

Aldoses and ketoses ('glycoses') provide a central metal with a considerable number of isomers that may act as chelators of variable denticity. Hence a glycose, though it is a single pure substance, reacts as a dynamic ligand library. In recent work, various metal probes such as $Pd^{II}N_2$-type fragments (N_2 = bidentate amine ligand), or M^{III}(tacn) residues (M = Co, Ga; tacn = 1,4,7-triazacyclononane), have been used to enrich those diolate or triolate species that are capable of forming chelates.[1–8] Among the metal probes, the $Pd^{II}N_2$-fragments are closely related to copper–ammine-based probes, which have played a significant role in the history of carbohydrate chemistry. In the middle of the last century, Reeves used them as a tool to unravel the conformation of the glycopyranoses. The method was based on the comparison of the specific rotations of a glycoside in water and in Schweizer's reagent. Reeves interpreted the presence or absence of marked differences as being indicative of either a specific conformation of the pyranoside or of dynamic behaviour, particularly in the $^4C_1 \Leftrightarrow {}^1C_4$ chair inversion.[9] Fluctuation between the two chair conformers is a common feature of some glycosides as well as their parent glycoses.[10] We may speculate that the capability of rapid chair inversion need not be lost on the formation of a metal chelate. To check this assumption experimentally, a considerable number of reliably assigned and precisely determined coupling constants should be available as the basis for a Karplus relationship treatment. To unravel the spectroscopic trace of the dynamics of a pyranose chelate, we introduced the new coordinating agent 'Pd-tmen'. This new reagent provided us with complete, high quality sets of $^3J_{H,H}$ coupling constants for a number of methyl aldopentopyranosides. This class of compounds seemed particularly suited to take a first step towards the investigation of fluctuating pyranose chelates because some of the free pentopyranosides are known to fluctuate (the lyxopyranoside and the ribopyranoside), whereas others do not (the arabinopyranoside and the xylopyranoside). Moreover, being glycosides rather than glycoses, the number of formed chelates should be limited for these chelators that are then well-suited for a first attempt.

2. Results and discussion

2.1. Pd-tmen: nomenclature and classification

The newly developed reagent 'Pd-tmen', an aqueous solution of [Pd^{II}(tmen)($OH)_2$] (tmen = *N*,*N*,*N*′,*N*′-tetramethyl-ethane-1,2-diamine), is a typical 'coordinating solvent'. Metal-containing reagents that had been developed primarily as cellulose solvents have been used as diagnostic tools for basic research on monosaccharides and derivatives thereof since the early days of carbohydrate chemistry. The first solvent of this kind was 'Schweizer's reagent' (1857), which is a solution of cupric hydroxide in excess aqueous ammonia.[11] In this work, Schweizer's reagent ('cuoxam', 'cuprammonium hydroxide', 'cupra') is abbreviated Cu-NH_3, using the nomenclature which has been introduced for cellulose

* Corresponding author. Fax: +89 2180 77407.
E-mail address: kluef@cup.uni-muenchen.de (P. Klüfers).

0008-6215/$ - see front matter © 2010 Elsevier Ltd. All rights reserved.
doi:10.1016/j.carres.2010.08.006

solvents. (In this nomenclature, M-L denotes an aqueous solution of the hydroxide of M, dissolved by a typical amount of L; if needed for differentiation, the molar ratio of M and L may be specified in the style 'Pd-2en' to denote a solution of $[Pd^{II}(en)_2](OH)_2$ in water [en = ethane-1,2-diamine], as well as the oxidation state of the metal).[12] Cu-NH_3 is a 'coordinating solvent' as it is capable of forming chelate complexes with a carbohydrate diol function after their deprotonation by the hydroxide equivalents. The formation of stable complexes has been demonstrated both by stability constant determinations and by crystal structure analysis.[7,13] Related solvents have been introduced, both coordinating such as Cu-en or Ni-tren and non-coordinating such as Cd-en ('cadoxen').[12,14–16] The latter class of cellulose solvents dissolves the polysaccharide by the action of strong base and bulky counterions similar to tetraalkylammonium hydroxide solvents but no coordination compound is formed.[12]

Six decades ago, Reeves was the first to use Cu-NH_3 as a tool for the conformational analysis of monosaccharides. As a result, he formulated instability criteria such as the axial-hydroxy-function count and the 'Δ2 effect' (an axial 2-OH together with an equatorial 1-OH), the latter implicitly including the later-recognised anomeric effect (Scheme 1, top right, shows an example).[17–20] In this work, we contrast Reeves's findings and conclusions with the results of our palladium complexation.

The first palladium-based solvents, Pd-en and Pd-NH_3, were introduced about a decade ago.[21,22] Because complexes formed are diamagnetic low-spin-d^8 species, Pd-en is an analytical tool that allows the use of NMR spectroscopy in complexation studies. A peculiarity of the palladium solvents is a key point in this work: the complexes are kinetically inert with respect to ligand exchange on the NMR timescale. NMR data that are mean values due to the contributions from two or more species (mean chemical shifts, mean coupling constants), are indicative of a dynamic behaviour of an individual intact complex. The NMR-detected conformational fluctuation of a palladium species thus is not explainable via a consecutive reaction path involving the free ligand such as: (1) dissociation of the complex, (2) conformational change of the free ligand and (3) re-metallation.

To collect a sufficient number of reliably assigned ^{13}C NMR signals and $^3J_{H,H}$ coupling constants, 2D NMR spectra free of cross-peak overlap are essential. Because mostly species-rich solutions are obtained, the cross-peak criterion is not always satisfied. To resolve this situation, a multi-probe approach seemed promising. Hence, data collected in Pd-en were supplemented with data from the related solvents. In this work, data from the Pd-chxn solvent, which contains the (*R*,*R*)-cyclohexane-1,2-diamine (chxn) ligand instead of en, were combined with data from the new solvent Pd-tmen.[4,23] The Pd-tmen solvent's characteristics are determined by the substitution of the N-bonded H atoms of Pd-en by methyl groups. As a result, there is (1) an increased steric demand in the direction of the bonded diolate and hence modified species stabilities and (2) no intramolecular hydrogen bonds can be formed toward adjacent functions of the bonded carbohydrate. A common property with other Pd-based solvents is the magnitude of the so-called 'coordination-induced shift' (CIS). Depending on the binding mode of the carbohydrate, these shifts remain almost constant among the solvents. Thus, in the case of five-membered chelate rings, the signals of the carbon atoms experience an approximately 10-ppm downfield shift relative to the free chelator. In the case of six-membered chelate rings, markedly smaller CISs are observed.[4,6,8,23,24] Finally, the practical benefits of using Pd-tmen in comparison with Pd-en and Pd-chxn should be mentioned, particularly Pd-tmen's markedly higher resistance to reduction to palladium(0). As a consequence, the ^1H NMR spectra, especially, are of a much higher quality and could be analysed in more detail. To minimise the amount of remaining free glycoside, all reactions in this work were performed under palladium(II)-excess conditions.

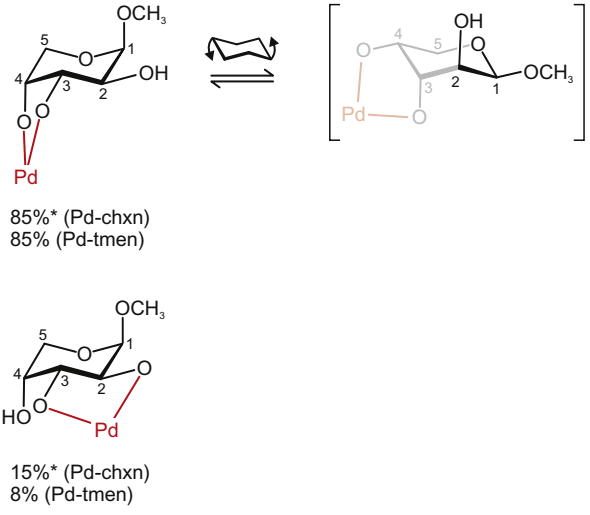

Scheme 1. Species detected in solutions of methyl β-D-arabinopyranoside in Pd-chxn and Pd-tmen at a molar Pd–glycoside ratio of 3:1. Percent values with an asterisk have been determined with β-L-arabinopyranoside and may thus slightly differ from the D enantiomer due to the chiral Pd-chxn probe. The top-right conformer was not observed. The formula's part drawn in black highlights one of Reeves's instability criteria, the 'Δ2 effect' (see text).

2.2. Methyl β-D- and β-L-arabinopyranoside

The methyl β-arabinopyranoside enantiomers are non-fluctuating in their free state but reside in the $^1C_4$ (D) or $^4C_1$ (L) conformation.[25,26] The formation of five-membered chelate rings by the attack of a vicinal diol function is the predominant mode of palladium(II)–pyranose binding. Both cis- or trans-diolate binding is common, the latter requiring a diequatorial conformation. As depicted in Scheme 1 for the D enantiomer, cis coordination is usually the preferred binding mode of methyl glycopyranosides. In the reaction of the methyl β-arabinopyranoside enantiomers with Pd-chxn and Pd-tmen, two kinds of complex species were thus detected in solution: the preferred cis-diolato complexes of the Me-β-Ara*p*3,4H$_{-2}$-κ$O^{3,4}$ enantiomers as the major, and the trans-diolato complexes of the Me-β-Ara*p*2,3H$_{-2}$-κ$O^{2,3}$ enantiomers as the minor species. Both palladium reagents form almost the same distribution of complex species in solution. The $^3J_{H,H}$ coupling constants indicate that the conformation of their respective free glycoside was maintained ($^1C_4$-D and $^4C_1$-L) on metallation (Table 1).

When attempting to crystallise one of the species, an unusual observation was made. As a rule of thumb, the major species of a solution equilibrium may be crystallised. The reason is the obvious similarity of parameters that are decisive for crystallisation such as nucleation energy and growth rate as well as the solubility of the species. As a result, the concentration usually determines the crystallising species. Contrary to these expectations, in the case of methyl β-L-arabinopyranoside, the minor species [Pd(*R*,*R*-chxn)(Me-β-L-Ara*p*2,3H$_{-2}$-κ$O^{2,3}$)] precipitates on oversaturation. Crystal structure analysis confirmed the coupling constant-derived spectroscopic assignment of the $^4C_1$ conformation. In terms of puckering parameters, the pyranose chair is almost undistorted (Fig. 1).[27]

Palladium binding seems to follow the same rules as the metallation by the ammine–copper(II) probe in the Cu-NH_3 solvent.[19] In the nomenclature used by Reeves, both the 2,3- as well as the 3,4-diol function produce *dextro* chelates, hence the overall *dextro* assignment in terms of Reeves's specific rotation values is compatible with the results on palladium (compare Scheme 1 for the

Table 1
Experimental and calculated $^{3}J_{H,H}$ values in Hz for the free glycoside and various metallated species of methyl β-arabinopyranoside[a]

	$^{3}J_{H1,H2}$	$^{3}J_{H2,H3}$	$^{3}J_{H3,H4}$	$^{3}J_{H4,H5eq}$	$^{3}J_{H4,H5ax}$	Conformation
Free D (exp.)[26]	2.8	10.0	3.0	2.3	1.0	$^{1}C_4$-D (Ref. 26)
L-κ$O^{2,3}$ (in Pd-chxn)	**3.2**	**10.3**	n.d.	n.d.	n.d.	**$^{4}C_1$-L (trans-vic.)**
L-κ$O^{3,4}$ (in Pd-chxn)	3.7	9.1	4.1	2.1	1.8	$^{4}C_1$-L (cis-vic.)
D-κ$O^{3,4}$ (in Pd-tmen)	3.5	9.1	4.2	2.2	1.8	$^{1}C_4$-D (cis-vic.)
1	**3.3**	**9.9**	**2.9**	**2.1**	**1.3**	**$^{4}C_1$-L (Karplus)**
D (idealised)	**3.2**	**9.6**	**3.2**	**2.5**	**0.6**	**$^{1}C_4$-D (Karplus)**
D (idealised)	**1.5**	**4.3**	**3.5**	**4.3**	**10.1**	**$^{4}C_1$-D (Karplus)**

[a] Bold: measured (formation of a *trans*-vicinal chelate) or calculated constants which unambiguously represent the specified conformer. For the calculation of constants, the Karplus relationship in Eq. 8 of Ref. 32 was used in conjunction with the torsion angles of an X-ray analysis or the angles of idealised structures (all torsions angles multiples of 60°).

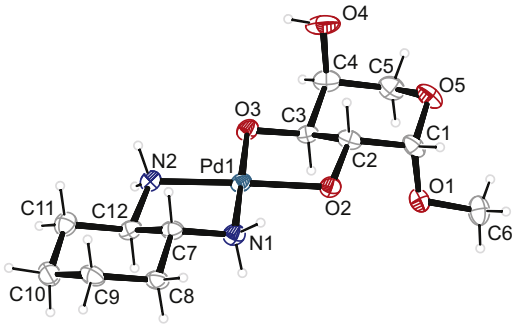

Figure 1. The molecular structure of [Pd(*R*,*R*-chxn)(Me-β-L-Ara*p*2,3H$_{-2}$-κ$O^{2,3}$)] in crystals of the dihydrate (**1**). ORTEP plot drawn with 50% probability ellipsoids. Interatomic distances (Å) and angles (°) (standard deviations of the last digit in parentheses): Pd1–O2 2.004(3), Pd1–O3 2.007(3), Pd1–N1 2.036(4), Pd1–N2 2.030(4); O2–Pd1–O3 86.06(14), N1–Pd1–N2 83.97(16); chelate torsion angles: O2–C2–C3–O3 52.6(5), N1–C7–C12–N2 −53.8(5); puckering parameters of the pyranose ring C1–C2–…: Q = 0.568(5) Å, θ = 3.5(5)°, φ = 134(9)°.[27]

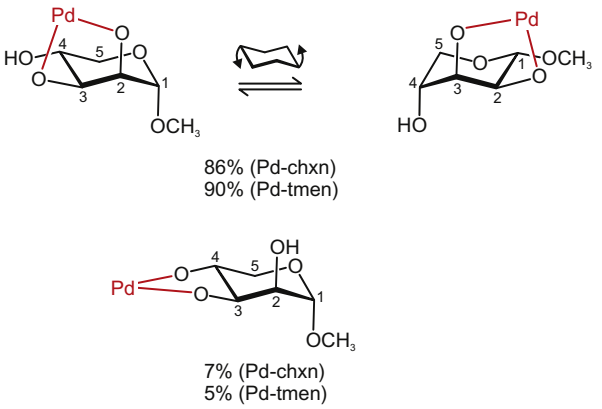

Scheme 2. Conformational fluctuation of the major κ$O^{2,3}$-binding methyl α-D-lyxopyranoside ligand in Pd-tmen and Pd-chxn at a molar 2:1 Pd–lyxopyranoside ratio. In Pd-tmen, the $^{4}C_1$ chair predominates over the $^{1}C_4$ conformer (7:3). The minor κ$O^{3,4}$-chelate was found in its only possible conformation.

nomenclature: when viewing through the Pd atom towards the pair of diol-carbon atoms, the two observed *dextro* chelates have the right O atom up and the left atom down; the non-observed chelate [Scheme 1, top right] is *levo* having its left O atom up and the right down. In contemporary IUPAC nomenclature, Reeves's *dextro* case is, unfortunately, a λ chelate, and Reeves's *levo* is δ [rule IR-9.3.4.14]).[28] As a historical note, Scheme 1 (top right) highlights Reeves's 'Δ2 effect' which burdens the depicted unobserved conformer. It should be noted at this point that Reeves considered diolate monoanions as the actual ligands instead of the dianions found in the solid state.[20]

2.3. Methyl α-D-lyxopyranoside

In contrast to methyl β-arabinopyranoside, free methyl α-D-lyxopyranoside fluctuates.[25,26] The reaction of methyl α-D-lyxopyranoside with the two palladium probes gave κ$O^{2,3}$-bonded Me-α-D-Lyx*p*2,3H$_{-2}$ as the major species accompanied by only small amounts of the trans-chelate Me-α-D-Lyx*p*3,4H$_{-2}$-κ$O^{3,4}$ (Scheme 2)—a result that underlines the predominance of diolate chelators derived from a cis-vicinal diol function. In the trans-equatorial minor species, fluctuation is frozen because only the $^{4}C_1$ conformer is able to act as a ligand. For the major species, however, the coupling constants from the Pd-tmen solvent confirmed an equilibrium between the $^{4}C_1$ and the $^{1}C_4$ conformation of the Me-α-D-Lyx*p*2,3H$_{-2}$-κ$O^{2,3}$ chelate. Of the two conformers, the $^{4}C_1$ chelate predominates (Table 2). Accordingly, structure analysis on yellow crystals of [Pd(*R*,*R*-chxn)(Me-α-D-Lyx*p*2,3H$_{-2}$)]·2.25H_2O (**2**) revealed the $^{4}C_1$ conformation. A detail of the pyranose puckering analysis is noteworthy. In two of the four molecules in the asymmetric unit, the angle θ is about 14° and 15°, which indicates an unusually large deviation from the chair conformation (the other θ angles in this work do not exceed ca. 6°). The phase angle points to an admixture of the E_5 conformation to the $^{4}C_1$ chair, which resembles a small distortion along the transitional path toward the $^{1}C_4$ chair (Fig. 2).[27]

Again, the result is compatible with that of the ammine–copper probe. Reeves interpreted a vanishing rotational shift, and, at the same time, a complex formation as confirmed by conductivity measurements in terms of the compensation of two $^{4}C_1$ *dextro* species (κ$O^{2,3}$ and κ$O^{3,4}$, namely the Cu analogues of the Pd species in Scheme 2 top left and bottom) and the *levo* $^{1}C_4$-κ$O^{2,3}$ complex (Scheme 2, top right).

2.4. Methyl β-D-ribopyranoside

Aqueous solutions of methyl β-D-ribopyranoside are characterised by the fluctuating glycoside's conformational equidistribution.[25,26] The coupling constants thus indicate a 1:1 mixture of the $^{4}C_1$ and the $^{1}C_4$ conformers of methyl β-D-ribopyranoside. The preferred cis-vicinal chelation is possible both for the κ$O^{2,3}$ and for the κ$O^{3,4}$ attacks on the metal probe. Accordingly, both kinds of species were observed in the respective solutions at about equal quantities (Scheme 3). The $^{3}J_{H,H}$ coupling constants of the complexes closely resemble those of the free ribopyranoside. Also, the [Pd(*R*,*R*-chxn)(Me-β-D-Rib*p*2,3H$_{-2}$-κ$O^{2,3}$)] as well as the [Pd(*R*,*R*-chxn)(Me-β-D-Rib*p*3,4H$_{-2}$-κ$O^{3,4}$)] chelates fluctuate (Table 3). The Pd-tmen probe produces the same fluctuating [Pd(tmen)(Me-β-D-Rib*p*2,3H$_{-2}$-κ$O^{2,3}$)] and [Pd(tmen)(Me-β-D-Rib*p*3,4H$_{-2}$-κ$O^{3,4}$)] species. The $^{3}J_{H,H}$ coupling constants show a slight dependence of the conformer quantities on the solvent (Table 3).

Table 2
Experimental and calculated $^{3}J_{H,H}$ values in Hz for the free glycoside and various metallated species of methyl α-D-lyxopyranoside[a]

	$^{3}J_{H1,H2}$	$^{3}J_{H2,H3}$	$^{3}J_{H3,H4}$	$^{3}J_{H4,H5eq}$	$^{3}J_{H4,H5ax}$	Conformation
Free (exp.)[26]	3.2	3.8	4.0	4.8	9.0	$^{4}C_1 \Leftrightarrow {}^{1}C_4$ (Ref. 26)
κ$O^{2,3}$ (in Pd-tmen)	3.6	4.0	6.7	3.8	7.2	$^{4}C_1 \Leftrightarrow {}^{1}C_4$, 7:3 ratio
κ$O^{3,4}$ (in Pd-tmen)	**1.6**	**3.2**	n.d.	n.d.	n.d.	**$^{4}C_1$ (trans-vic.)**
2	**1.7**	**4.5**	**8.4**	**4.7**	**10.1**	**$^{4}C_1$ (Karplus)**
Idealised major	**1.8**	**3.5**	**9.6**	**4.3**	**10.1**	**$^{4}C_1$ (Karplus)**
Idealised minor	**8.1**	**3.5**	**4.3**	**2.5**	**0.6**	**$^{1}C_4$ (Karplus)**

[a] See the footnote of Table 1 for more details.

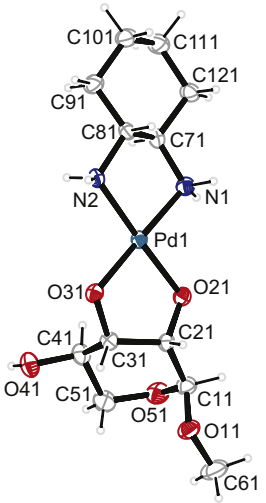

Figure 2. The molecular structure of [Pd(*R*,*R*-chxn)(Me-α-D-Lyx*p*2,3H$_{-2}$)] in crystals of the 2.25-hydrate (**2**). ORTEP plot drawn with 50% probability ellipsoids. Interatomic distances (Å) and angles (°) in the four molecules of the asymmetric unit (standard deviations of the last digit in parentheses): Pd1 to: O21 1.961(3), O31 2.007(3), N1 2.045(4), N2 2.048(4), Pd2 to: O22 1.983(3), O32 1.993(3), N4 2.031(5), N3 2.032(4), Pd3 to: O33 2.000(3), O23 2.003(3), N6 2.029(4), N5 2.046(4), Pd4 to: O24 1.988(3), O34 2.003(3), N7 2.038(4), N8 2.048(4); O21–Pd1–O31 84.73(13), O22–Pd2–O32 84.85(13), O23–Pd3–O33 84.42(12), O24–Pd4–O34 84.74(12); chelate torsion angles: O21–C21–C31–O31 −45.6(5), O22–C22–C32–O32 −46.2(5), O23–C23–C33–O33 −50.6(5), O24–C24–C34–O34 −52.5(5); puckering parameters of the pyranose rings: O51–C11–…: Q = 0.522(5) Å, θ = 13.9(7)°, φ = 310(2)°; O52–C12–…: Q = 0.552(5) Å, θ = 15.2(6)°, φ = 297(2)°; O53–C13–…: Q = 0.549(5) Å, θ = 5.8(5)°, φ = 302(6)°; O54–C14–…: Q = 0.540(5) Å, θ = 6.1(5)°, φ = 269(5).[27]

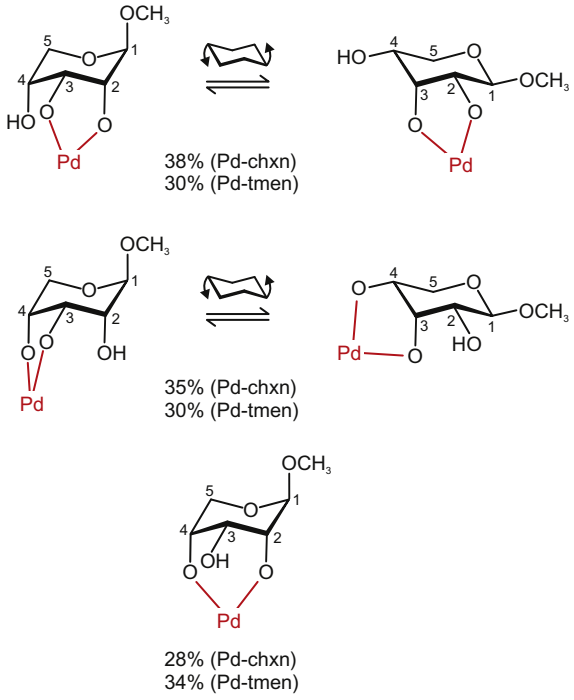

Scheme 3. Conformational fluctuation of both the κ$O^{2,3}$- and the κ$O^{3,4}$-binding methyl β-D-ribopyranoside ligand in Pd-tmen and Pd-chxn at a molar 2:1 Pd–ribopyranoside ratio. The κ$O^{2,4}$-chelate (bottom) adopts its only possible conformation.

Unlike the arabinopyranoside and the lyxopyranoside, the ribopyranoside provides a special bonding mode to the palladium(II) central metal. For the ribopyranoside, trans-vicinal diol bonding is not possible and is replaced by an alternative that the former glycosides are lacking: the formation of six-membered chelate rings by *syn*-diaxial κ$O^{2,4}$ bonding. In the past, few compounds with this bonding mode have been characterised, among them is the sterically restricted pyranoidic dianion derived from levoglucosan as well as some furanose ligands.[4,6,21] In a recent work, our group attributed the intrinsic stability to this mode for simple pyranoses as well. Hence, dimetalled β-D-xylopyranose was found to adopt its all-axial $^{1}C_4$ conformation in a κ$O^{1,3}$:κ$O^{2,4}$-bonded dinuclear complex.[4] In fact, the κ$O^{2,4}$-bonded methyl β-D-ribopyranoside chelator was detected by both probes. [Pd(*R*,*R*-chxn)(Me-β-D-Rib*p*2,4H$_{-2}$-κ$O^{2,4}$)] as well as its tmen analogue show a pattern of coordination-induced shifts which is substantially different from vicinal chelation (Tables 5 and 6). The results are in fair agreement with CISs of the [Pd(en)(1,6AnGlc2,4H$_{-2}$-κ$O^{2,4}$)] (1,6AnGlc = 1,6-anhydro-β-D-glucose, 'levoglucosan') complex.[21] However, a caveat on CIS values should be noted. On the one hand, levoglucosan, a conformationally fixed bicyclic molecule, does not alter its shape markedly on coordination. Methyl β-D-ribopyranoside, on the other hand, is fluctuating in its non-bonded standard state, but is fixed in the κ$O^{2,4}$-bonded chelate. Consequently, the CIS values are not affected solely by the coordination of palladium(II) (as is implied in the term *coordination*-induced shift), but are biased by a component caused by freezing out one conformer. As a result, unsystematic shift differences appear for all carbon atoms in Table 5 and 6.

Attempts to isolate one of the three species of roughly equal quantity led, fortunately, to crystals of the lastly described kind, [Pd(*R*,*R*-chxn)(Me-β-D-Rib*p*2,4H$_{-2}$-κ$O^{2,4}$)]. The structural analysis (Fig. 3) confirmed the spectroscopic assignment also for this species which lacked the unambiguous CIS values typical for vicinal diol chelation. The pyranose pucker is normal for this bonding mode with its slightly distorted $^{1}C_4$ chair conformation.

As expected, the manifold binding modes of the ribopyranoside were beyond the analytical power of the simple method that was available to Reeves in his 1950 work. Because, using this method, a κ$O^{2,4}$ species is silent (as Reeves demonstrated for the case of levoglucosan) and all other species have a *dextro–levo* couple, there was no chance to differentiate between the compensation of effects within an individual conformer and fluctuating behaviour. Reeves's conclusion of a compensating couple of $^{4}C_1$-κ$O^{2,3}$ and $^{4}C_1$–κ$O^{3,4}$ complexes was thus not based on experimental data but on an instability criterion which has been re-evaluated

Table 3
Experimental and calculated $^3J_{H,H}$ values in Hz for the free glycoside and various metallated species of methyl β-D-ribopyranoside[a]

	$^3J_{H1,H2}$	$^3J_{H2,H3}$	$^3J_{H3,H4}$	$^3J_{H4,H5eq}$	$^3J_{H4,H5ax}$	Conformation
Free (exp.)[26]	5.1	3.4	3.4	3.5	7.0	$^4C_1 \Leftrightarrow {}^1C_4$ (Ref. 26)
κO^{2,3} (Pd-chxn)	5.2	3.3	3.3	n.d.	n.d.	$^4C_1 \Leftrightarrow {}^1C_4$, 5:5 ratio
κO^{3,4} (Pd-chxn)	6.0	2.7	3.3	4.4	7.4	$^4C_1 \Leftrightarrow {}^1C_4$, 7:3 ratio
κO^{2,3} (Pd-tmen)	3.5	3.6	3.6	–	–	$^4C_1 \Leftrightarrow {}^1C_4$, 3:7 ratio
κO^{3,4} (Pd-tmen)	4.5	3.0	3.2	3.0	5.0	$^4C_1 \Leftrightarrow {}^1C_4$, 4:6 ratio
κO^{2,4} (Pd-chxn)	**1.4**	**3.8**	**3.6**	**1.6**	**1.9**	**$^1C_4$ (*syn*-diaxial)**
κO^{2,4} (Pd-tmen)	**1.8**	**3.7**	**3.7**	**1.6**	**2.0**	**$^1C_4$ (*syn*-diaxial)**
3	**2.3**	**2.9**	**3.0**	**1.7**	**4.0**	**$^1C_4$ (Karplus)**
Idealised	**1.8**	**3.5**	**3.2**	**2.5**	**0.6**	**$^1C_4$ (Karplus)**
Idealised	**8.1**	**3.5**	**3.5**	**4.3**	**10.1**	**$^4C_1$ (Karplus)**

[a] See the footnote of Table 1 for more details.

Table 4
Experimental and calculated $^3J_{H,H}$ values in Hz for the free glycoside and various metallated species of methyl β-D-xylopyranoside[a]

	$^3J_{H1,H2}$	$^3J_{H2,H3}$	$^3J_{H3,H4}$	$^3J_{H4,H5eq}$	$^3J_{H4,H5ax}$	Conformation
Free (exp.)	7.9	9.5	9.5	5.5	11.0	$^4C_1$ (Ref. 26)
κO^{2,3} (in Pd-chxn)	**7.7**	**9.3**	**10.4**	**5.3**	**10.2**	**$^4C_1$ (trans-vic.)**
κO^{3,4} (in Pd-chxn)	**7.4**	**9.3**	**9.1**	**4.7**	n.d.	**$^4C_1$ (trans-vic.)**
κO^{2,3} (in Pd-tmen)	**7.8**	**9.5**	**8.9**	**5.4**	**10.0**	**$^4C_1$ (trans-vic.)**
κO^{3,4} (in Pd-tmen)	**7.6**	**9.2**	**9.3**	**4.7**	**10.4**	**$^4C_1$ (trans-vic.)**
4	**7.9**	**9.6**	**9.4**	**4.2**	**10.1**	**$^4C_1$ (Karplus)**
5-κO^{2,3}	**7.9**	**9.4**	**9.4**	**4.1**	**10.1**	**$^4C_1$ (Karplus)**
5-κO^{3,4}	**7.8**	**9.3**	**9.5**	**4.4**	**10.1**	**$^4C_1$ (Karplus)**
Idealised	**8.1**	**9.8**	**9.6**	**4.3**	**10.1**	**$^4C_1$ (Karplus)**
κO^{2,4} (in Pd-tmen)	**<2**	**<2**	**<2**	**1.2**	**1.2**	**$^1C_4$ (*syn*-diaxial)**
Idealised	**1.8**	**4.3**	**4.3**	**2.5**	**0.6**	**$^1C_4$ (Karplus)**

[a] See the footnote of Table 1 for more details.

Table 5
^{13}C NMR chemical shifts (δ) and shift differences ($\Delta\delta$) to the free pentopyranoside of methyl pentopyranosides in Pd-chxn

		C1	C2	C3	C4	C5	CH_3	Chelate
Me-β-L-Ara*p*2,3H$_{-2}$	δ	102.0	77.8	76.4	71.5	63.2	55.4	
	$\Delta\delta$	1.5	9.0	7.0	2.0	0.1	−0.4	κO^{2,3}
Me-β-L-Ara*p*3,4H$_{-2}$	δ	100.8	71.8	78.4	78.7	62.6	55.6	
	$\Delta\delta$	0.3	3.0	9.0	9.2	−0.5	−0.2	κO^{3,4}
Me-α-D-Lyx*p*2,3H$_{-2}$	δ	104.0	79.9	81.1	70.5	63.8	56.4	
	$\Delta\delta$	2.2	9.8	9.9	3.0	0.7	0.5	κO^{2,3}
Me-α-D-Lyx*p*3,4H$_{-2}$	δ	101.8	72.8	80.9	74.5	64.4	55.4	
	$\Delta\delta$	0.0	2.7	9.7	7.0	1.3	−0.5	κO^{3,4}
Me-β-D-Rib*p*2,3H$_{-2}$	δ	103.6	80.5	77.9	68.1	63.5	56.5	
	$\Delta\delta$	1.6	9.8	9.6	−0.2	0.1	−0.2	κO^{2,3}
Me-β-D-Rib*p*3,4H$_{-2}$	δ	102.2	70.4	77.9	77.6	64.7	56.6	
	$\Delta\delta$	0.2	−0.3	9.6	9.3	1.1	−0.1	κO^{3,4}
Me-β-D-Rib*p*2,4H$_{-2}$	δ	103.9	67.2	67.6	65.9	65.6	55.1	
	$\Delta\delta$	1.9	−3.5	−0.7	−2.4	2.0	−1.6	κO^{2,4}
Me-β-D-Xyl*p*2,3H$_{-2}$	δ	105.6	82.2	85.8	71.2	66.2	57.2	
	$\Delta\delta$	1.0	8.6	9.5	1.4	0.5	−0.6	κO^{2,3}
Me-β-D-Xyl*p*3,4H$_{-2}$	δ	104.9	74.7	85.8	79.2	65.4	57.6	
	$\Delta\delta$	0.3	1.1	9.5	9.4	−0.3	−0.2	κO^{3,4}

recently (1,3-syndiaxial hydroxy groups being not too destabilising).[29,30]

2.5. Methyl β-D-xylopyranoside

Methyl β-D-xylopyranoside is found in the $^4C_1$ conformation with four equatorial substituents. Conformational fluctuation is also not expected to be induced by metallation because a fluctuating pentoside chelate obviously requires a cis-vicinal diol function. In a series of the four pentoses, α- and β-xylopyranoside are the only potential ligands that lack this structural feature. Instead, two trans-vicinal diol sites can attack the metal probes. Due to the similarity of the κ$O^{2,3}$ and the κ$O^{3,4}$ sites—an analogy to the ribopyranoside which provides two cis-vicinal diol functions—equipartition of the chelates may be expected. In fact, Pd-chxn enriched solutions of methyl β-D-xylopyranoside with almost equal amounts of the conformationally fixed complexes [Pd(*R*,*R*-chxn)(Me-β-D-Xyl*p*2,3H$_{-2}$-κ$O^{2,3}$)] and the κ$O^{3,4}$-bonded isomer (Scheme 4).

The result obtained with the Pd-tmen probe was unexpected but may be rationalised by the experience that trans-vicinal chelation is a second-choice coordination mode. At a quantity of 13%, the chair-inverted species [Pd(tmen)(Me-β-D-Xyl*p*2,4H$_{-2}$-κ$O^{2,4}$)] was detected in addition to the two major species of the Pd-chxn probe (Scheme 4). The assignment depends on the coupling-constant analysis (Table 4). Because the conformation is different from that of the standard state of the free glycoside, CIS values in this case are meaningless (Table 6). This result underlines the stability

Table 6
^{13}C NMR chemical shifts (δ) and shift differences ($\Delta\delta$) to the free pentopyranoside of methyl pentopyranosides in Pd-tmen

		C1	C2	C3	C4	C5	OCH_3	Chelate
Me-β-D-Ara*p*2,3H$_{-2}$	δ	102.2	78.1	77.2	72.0	63.2	55.8	
	$\Delta\delta$	1.7	9.3	7.8	2.5	0.1	0.0	κ$O^{2,3}$
Me-β-D-Ara*p*3,4H$_{-2}$	δ	101.1	72.3	78.6	79.1	63.0	55.9	
	$\Delta\delta$	0.6	3.5	9.2	9.6	−0.1	0.1	κ$O^{3,4}$
Me-α-D-Lyx*p*2,3H$_{-2}$	δ	104.0	79.9	81.1	70.5	63.8	56.4	
	$\Delta\delta$	2.2	9.8	9.9	3.0	0.7	0.5	κ$O^{2,3}$
Me-α-D-Lyx*p*3,4H$_{-2}$	δ	101.8	72.8	80.9	74.5	64.4	55.4	
	$\Delta\delta$	0.0	2.7	9.7	7.0	1.3	−0.5	κ$O^{3,4}$
Me-β-D-Rib*p*2,3H$_{-2}$	δ	103.8	81.3	75.7	69.3	64.0	56.4	
	$\Delta\delta$	1.8	10.6	7.4	1.0	0.4	−0.3	κ$O^{2,3}$
Me-β-D-Rib*p*3,4H$_{-2}$	δ	102.8	70.9	67.0	78.7	65.0	56.5	
	$\Delta\delta$	0.8	0.2	7.7	10.4	1.4	−0.2	κ$O^{3,4}$
Me-β-D-Rib*p*2,4H$_{-2}$	δ	104.3	69.1	67.6	67.8	65.7	55.3	
	$\Delta\delta$	2.3	−1.6	−0.7	−0.5	2.1	−1.4	κ$O^{2,4}$
Me-β-D-Xyl*p*2,3H$_{-2}$	δ	105.8	82.8	86.4	71.6	66.5	57.4	
	$\Delta\delta$	1.2	9.2	10.1	1.8	0.8	−0.4	κ$O^{2,3}$
Me-β-D-Xyl*p*3,4H$_{-2}$	δ	105.4	75.1	86.2	79.6	65.8	58.0	
	$\Delta\delta$	0.8	1.5	9.9	9.8	0.1	0.2	κ$O^{3,4}$
Me-β-D-Xyl*p*2,4H$_{-2}$	δ	103.1	71.7	68.8	68.5	60.8	55.6	
	$\Delta\delta$	−1.5	−1.9	−7.5	−1.3	−4.9	−2.2	κ$O^{2,4}$

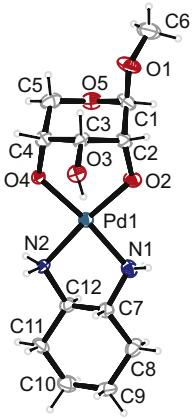

Figure 3. The molecular structure of [Pd(*R*,*R*-chxn)(Me-β-D-Rib*p*2,4H$_{-2}$-κ$O^{2,4}$)] in crystals of the trihydrate (**3**). ORTEP plot drawn with 50% probability ellipsoids. Interatomic distances (Å) and angles (°) (standard deviations of the last digit in parentheses): Pd1–O2 1.998(7), Pd1–O4 2.006(7), Pd1–N1 2.039(9), Pd1–N2 2.045(8); O2–Pd1–O4 95.1(3), N1–Pd1–N2 83.3(4); torsion angles: O2–C2–C3–O3 57.4(9), O3–C3–C4–O4 −59.5(9), N1–C7–C12–N2 −54.6(7); puckering parameters of the pyranose ring C1–C2–…: Q = 0.556(10) Å, θ = 176.8(9)°.[27]

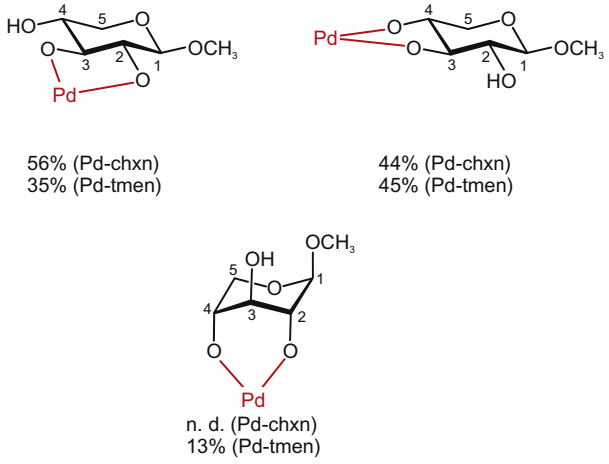

Scheme 4. Frozen conformations in all monometallated isomers of methyl β-D-xylopyranoside.

of the six-ring chelates. Despite the fact that all substituents are axial in methyl $^1C_4$-β-D-xylopyranoside, sufficient stability is gained by palladium-binding to make the species detectable.

The spectroscopic results on the major species are supported by X-ray analysis. From Pd-chxn batches, [Pd(*R*,*R*-chxn)(Me-β-D-Xyl*p*2,3H$_{-2}$-κ$O^{2,3}$)]·2.5H$_2$O (**4**) crystallizes. The complex molecules show almost undistorted $^4C_1$ chairs (Fig. 4). With Pd-tmen, the two major monometallated isomers, [Pd(tmen)(Me-β-D-Xyl*p*2,3H$_{-2}$-κ$O^{2,3}$)] and its κ$O^{3,4}$-bonded analogue, co-crystallise. Again, almost undistorted $^4C_1$ chairs are found in agreement with the spectroscopic result (Fig. 5).

In terms of specific rotation values in Cu-NH_3, Reeves reported a compensating couple of *dextro* and *levo* chelation.[19] This result is in-line with roughly equal quantities of κ$O^{2,3}$- (*levo*) and κ$O^{3,4}$-bonding (*dextro*).

3. Conclusions

Glycoses (aldoses and ketoses) provide a metal probe with a dynamic ligand library by adopting various configurations and conformations. The most powerful tool to unravel both the configuration and the conformation of a metal-chelating glycose isomer is NMR spectroscopy, particularly the Karplus relationship-based analysis of coupling constants. Usually, a metallated glycose species (as well as the free glycose) has a well-defined con-

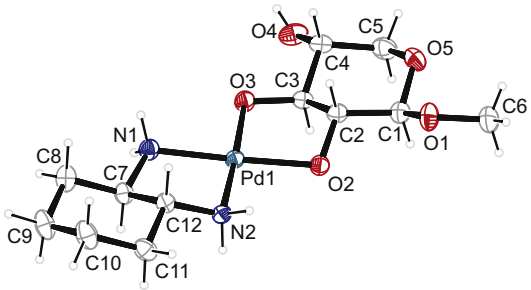

Figure 4. The molecular structure of [Pd(*R*,*R*-chxn)(Me-β-D-Xyl*p*2,3H$_{-2}$-κ$O^{2,3}$)] in crystals of the 2.5-hydrate (**4**). ORTEP plot drawn with 50% probability ellipsoids. Interatomic distances (Å) and angles (°) (standard deviations of the last digit in parentheses): Pd1–O2 2.014(2), Pd1–O3 2.019(3), Pd1–N1 2.041(3), Pd1–N2 2.020(3); O2–Pd1–O3 85.43(9), N1–Pd1–N2 83.12(11); chelate torsion angles: O2–C2–C3–O3 55.3(3), N1–C7–C12–N2 −52.1(3). Puckering parameters of the pyranose ring C1–C2–…: Q = 0.579(4) Å, θ = 2.4(4)°.[27]

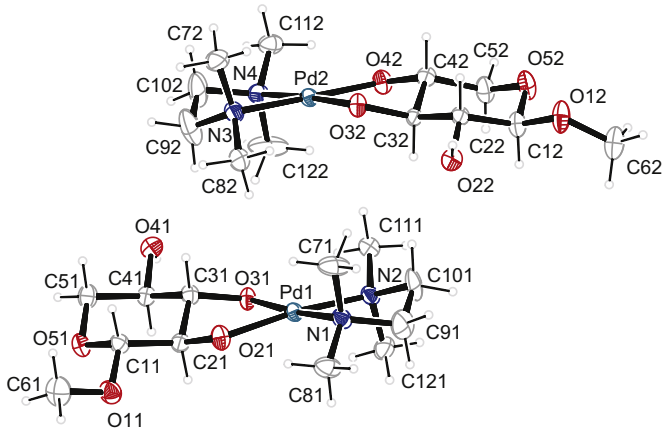

Figure 5. The asymmetric unit (water molecules omitted) of [Pd(tmen)(Me-β-D-Xyl*p*2,3H$_{-2}$-κ$O^{2,3}$)][Pd(tmen)(Me-β-D-Xyl*p*3,4H$_{-2}$-κ$O^{3,4}$)]·H_2O (**5**). ORTEP plot drawn with 50% probability ellipsoids. Interatomic distances (Å) and angles (°) (standard deviations of the last digit in parentheses): Pd1–O21 2.004(3), Pd1–O31 2.000(2), Pd1–N1 2.079(3), Pd1–N2 2.055(3), Pd2–O32 1.9945(19), Pd2–O42 2.001(3), Pd2–N3 2.064(3), Pd2–N4 2.067(3); O21–Pd1–O31 85.73(13), N1–Pd1–N2 86.01(17), O32–Pd2–O42 85.86(13), N3–Pd2–N4 85.75(17); chelate torsion angles: O21–C21–C31–O31 57.6(4), O32–C32–C42–O42 −55.4(4), N1–C91–C101–N2 −53.2(5), N3–C92–C102–N4 55.3(5). Puckering parameters of the pyranose rings: O51–C11–…: Q = 0.576(4) Å, θ = 4.4(4)°; O52–C12–…: Q = 0.564(4) Å, θ = 3.4(4)°.[27]

figuration and conformation and the interpretation of its typical NMR signal set is straightforward. In fact, the dynamic behaviour of some pyranoses such as ribopyranose and lyxopyranose is less common and might be thought of as frozen upon metal chelation. This assumption definitely holds true, for example, for the incorporation of a trans-diequatorial diol function such as the κ$O^{3,4}$ site of lyxopyranose in a chelate ring, which prevents this function from transitioning to the diaxial conformer. However, evidence was collected in this work for the maintenance of a pyranose's conformational fluctuation in the case of a cis-vicinal chelator. We investigated the spectroscopic trace of conformational fluctuation of this type in a couple of aldopentopyranosides as the basis for a discussion of the possible dynamic behaviour of similar chelates formed by the parent glycoses. As a prerequisite for obtaining a set of reliable coupling constants of a metallated pyranoside, we introduced a new cellulose solvent, Pd-tmen, thus expanding the sparse data from other solvents in a step towards a multi-probe strategy. As a result, for cis-vicinal diol functions, anellation of a chelate and a pyranose ring does not freeze the interconversion of the two chair conformers in terms of NMR spectroscopy. Instead, intermediate coupling constants can serve as a measure of the conformational equilibrium's position. In agreement with the number of cis-vicinal diol functions, the investigated methyl pyranosides of lyxose, ribose and xylose exhibit one, two and zero fluctuating palladium(II) chelates, respectively.

A second topic is addressed in this work. The observation of a stable, binuclear bis-chelate of the formula [{Pd(*R*,*R*-chxn)}$_2$($^1C_4$-β-D-Xyl*p*H$_{-4}$-κ$O^{1,3}$:κ$O^{2,4}$)], which is derived from the dimetallated $^1C_4$-all-axial conformer of β-D-xylopyranose, led to the issue of *syn*-diaxial pyranose chelation. We detected this chelation mode for the complexes of two pentosides: [PdN_2(Me-β-D-Rib*p*2,4H$_{-2}$)] (N_2 = chxn, tmen) and [Pd(tmen)(Me-β-D-Xyl*p*2,4H$_{-2}$)]. The formation of six-membered chelate rings results in the absence of pronounced coordination-induced shifts. Moreover, the expected small shifts are biased by a conformational change. Thus, both pentosides are fixed in their $^1C_4$ conformer, which resembles a freezing of the ribopyranoside fluctuation and the inversion of the xylopyranoside chair. Hence, in both cases, the standard state of the CIS calculation is different from the chelating conformation, an effect that is more pronounced for the xylopyranoside and less so in case of the ribopyranoside. Accordingly, the tabulated Δδ values (Tables 5 and 6) provide a typical example of the failure to derive a metal-binding site on the mere basis of CIS values.

We mentioned our appreciation of Reeves's historical contribution to our knowledge of the pyranoses' conformation in the Section 2. Keeping in mind the limitations of Reeves's method, his analysis of the arabinopyranoside, the lyxopyranoside and the xylopyranoside was correct—only the complicated ribopyranoside case was not (and could not be) correctly assigned.

4. Experimental

4.1. Methods and materials

Reagent grade chemicals were purchased from ABCR, Euriso–Top, Fluka, Glycon, Merck, Omicron, Sigma–Aldrich and TCI were used as supplied. The synthesis of [Pd(*R*,*R*-chxn)Cl_2] relies on a published procedure.[31] The syntheses of [Pd(*R*,*R*-chxn)$(OH)_2$] and [Pd(tmen)$(OH)_2$] were carried out under a nitrogen atmosphere using standard Schlenk techniques. All Pd–carbohydrate complexes were prepared in air and ice-bath cooling. To obtain crystals of good quality, crystallisation was interrupted typically at a yield of 10–20%. Elemental analyses were collected on an Elementar Vario EL Apparatur.

4.2. NMR spectroscopy

NMR spectra were recorded at room temperature on a Jeol Eclipse 400 (^{1}H: 400 MHz, ^{13}C{^{1}H}: 101 MHz) NMR or a Jeol 500 Eclipse spectrometer (^{1}H: 500.16 MHz; ^{13}C{^{1}H}: 125.77 MHz) spectrometers. The signals of the deuterated solvent (^{13}C{^{1}H}) and the residual protons therein (^{1}H) were used as an internal secondary reference for the chemical shift. When D_2O was used as a solvent, either a drop of methanol (referenced to 49.5 ppm) or a small capillary tube containing DMSO-d_6 was added to the sample tube (5 mm) in order to obtain a reference signal in the ^{13}C{^{1}H} NMR spectra. When necessary, the ^{1}H and ^{13}C{^{1}H} NMR signals were assigned by means of ^{1}H–^{1}H-COSY, DEPT135, ^{1}H–^{13}C-HMQC and ^{1}H–^{13}C-HMBC experiments in solutions of [Pd(*R*,*R*-chxn)$(OD)_2$] (0.5 M) in D_2O. Shift differences are given as $\delta(C_{complex}) - \delta(C_{free\ sugar})$. The values for the free sugars were determined in neutral aqueous solution and were referenced to 49.5 ppm for the $_{13}$C NMR signal of methanol. The percentage of the individual species in the solution equilibrium as given in the schemes was determined by the integration of the ^{1}H NMR spectra, or, if no signals free of overlap were found, by the integration of the C1 signals in the ^{13}C NMR spectra. Conformational analysis was based on Karplus relationships applied to $^3J_{H,H}$ coupling constants.[32]

4.3. Synthesis of palladium reagents

4.3.1. [Pd(*R*,*R*-chxn)Cl_2]

To a suspension of $PdCl_2$ (5.00 g, 0.3 mol) in 50 mL of water, KCl (4.20 g, 0.6 mol) was added at 45 °C and stirred for 10 min until a brown solution of K_2PdCl_2 was formed. A solution of (1*R*,2*R*)-cyclohexane-1,2-diamine (3.22 g, 0.3 mol) dissolved in 100 mL of 0.5 m HCl was slowly added. After the reaction mixture was stirred for 1 h at 45 °C, the pH was adjusted with dilute NaOH (1 m) to pH 7.0, and the yellow complex precipitated from the solution. The reaction mixture was stirred for another 3 h at 45 °C, and the pH was controlled in the first hour. After the suspension was cooled to room temperature the yellow complex was filtered, washed with cold water and was dried in vacuo over $CaCl_2$ (7.81 g, yield 95 %). Anal. Calcd for $C_6H_{14}Cl_2N_2Pd$: C, 24.72; H, 4.84; N, 9.61; Cl, 24.32. Found: C, 24.64; H, 4.78; N, 9.57; Cl, 24.20. ^{13}C{^{1}H} NMR (100.63 MHz, DMSO-d_6): δ 23.7 (2C, γ-CH_2), 32.2 (2C, β-CH_2), 61.0 (2C, α-CH_2).

4.3.2. [Pd(*R*,*R*-chxn)(OH)$_2$] (*c* = 0.3 M)

[Pd(R,R-chxn)Cl$_2$] (1.75 g, 6.00 mmol), Ag$_2$O (1.45 g, 6.26 mmol) and water (20 mL) were stirred under nitrogen with exclusion of light at 40 °C. After 2 h AgCl was removed by filtration through G4 filter under nitrogen atmosphere, leaving a yellow solution. Solutions of higher or lower concentration were prepared by varying the amount of water. For the preparation of [Pd(*R*,*R*-chxn)(OD)$_2$], D$_2$O was used. The alkaline [Pd(*R*,*R*-chxn)(OH)$_2$] solution (pH 12 at a concentration of 0.3 M) was kept under nitrogen at 4 °C to prevent absorption of carbon dioxide. ^{1}H NMR (400.18 MHz, D$_2$O): δ 1.02–1.21 (m, 4H, β-CH$_2$, γ-CH$_2$), 1.56–1.59 (m, 2H, γ-CH$_2$), 1.90–1.93 (m, 2H, β-CH$_2$), 2.32–2.35 (m, 2H, α-CH$_2$). ^{13}C{^{1}H} NMR (100.63 MHz, D$_2$O): δ 23.6 (2C, γ-CH$_2$), 33.0 (2C, β-CH$_2$), 60.2 (2C, α-CH$_2$). ^{13}C{^{1}H} NMR (100.63 MHz, H$_2$O): δ 24.0 (2C, γ-CH$_2$), 33.5 (2C, β-CH$_2$), 60.9 (2C, α-CH$_2$).

4.3.3. [Pd(tmen)Cl$_2$]

To a suspension of PdCl$_2$ (5.00 g, 28.2 mmol) in water (85 mL) was added HCl (5.00 mL, 0.5 M), and the mixture was stirred for 10 min until a brown solution was formed. With stirring, on dropwise addition of *N*,*N*,*N*′,*N*′-tetramethylethane-1,2-diamine (6.04 g, 52.0 mmol) in water (15 mL) a yellow precipitate formed. After stirring for 30 min, the yellow complex was filtered through a G4 filter, washed with cold water and was dried in vacuo. The yield was 7.68 g (93%). Anal. Calcd for $C_6H_{16}Cl_2N_2Pd$: C, 24.55; H, 5.49; N, 9.54; Cl, 24.16. Found: C, 24.37; H, 5.36; N, 9.50; Cl, 24.12.

4.3.4. [Pd(tmen)(OH)$_2$] (*c* = 0.45 M)

[Pd(tmen)Cl$_2$] (3.30 g, 11.24 mmol), Ag$_2$O (2.80 g, 12.08 mmol) and water (25 mL) were stirred under nitrogen with exclusion of light at 40 °C. After 30 min AgCl was removed by filtration through a G4 filter under nitrogen atmosphere, leaving a yellow solution. For the preparation of [Pd(tmen)(OD)$_2$], D$_2$O was used. The alkaline [Pd(tmen)(OH)$_2$] solution was kept under a nitrogen atmosphere at 4 °C to prevent absorption of carbon dioxide. ^{13}C{^{1}H} NMR (100.63 MHz, D$_2$O): δ 49.7 (4C, CH$_3$), 61.5 (2C, CH$_2$).

4.4. Synthesis of methyl pentoside complexes

For NMR investigation, the methyl pentosides were dissolved in 1 mL of Pd-chxn (H$_2$O, 0.3 M/D$_2$O, 0.5 M) or Pd-tmen (D$_2$O, 0.45 M) at a molar 2:1 ratio of Pd and glycoside (3:1 for methyl β-L-arabinopyranoside) and were stirred for 12 h at 4 °C to guarantee a high degree of conversion.

4.4.1. (1*R*,2*R*)-Cyclohexane-1,2-diamine(methyl β-L-arabinopyranos-2,3-*O*-diato)palladium(II) dihydrate

Methyl β-L-arabinopyranoside (74.0 mg, 0.45 mmol) was dissolved in [Pd(*R*,*R*-chxn)(OH)$_2$] (4.5 mL, 0.3 M, 0.135 mmol), and stirred for 2 h at 4 °C. 0.2 mL cold water and 6.85 mL cold acetone were added to 1 mL of the solution. After 2 days, the solution was covered with a layer of 3 mL isopropanol. Yellow crystals were formed within 10 days at 5 °C.

4.4.2. (1*R*,2*R*)-Cyclohexane-1,2-diamine(methyl α-D-lyxopyranos-2,3-*O*-diato)palladium(II) 2.25-hydrate

Methyl α-D-lyxopyranoside (213.0 mg, 0.13 mmol) was dissolved in [Pd(*R*,*R*-chxn)(OH)$_2$] (1 mL, 0.26 M, 0.26 mmol), and stirred for 2 h at 4 °C. The solution was saturated with acetone. Subsequently, acetone vapours were allowed to diffuse into the solution. Pale yellow crystals were formed within 1 day at 5 °C.

4.4.3. (1*R*,2*R*)-Cyclohexane-1,2-diamine(methyl β-D-ribopyranos-2,4-*O*-diato)palladium(II) trihydrate

Methyl β-D-ribopyranoside (82.0 mg, 0.5 mmol) was dissolved in [Pd(*R*,*R*-chxn)(OH)$_2$] (5 mL, 0.3 M, 0.15 mmol), and stirred for

Table 7
Crystallographic data for **1**–**3**

	1	**2**	**3**
Empirical formula	$C_{12}H_{28}N_2O_7Pd$	$C_{12}H_{28.50}N_2O_{7.25}Pd$	$C_{12}H_{30}N_2O_8Pd$
M_r [g mol^{-1}]	418.78	423.27	436.80
Crystal size [mm]	0.14 × 0.14 × 0.13	0.191 × 0.065 × 0.023	0.27 × 0.07 × 0.02
Crystal system	Orthorhombic	Triclinic	Monoclinic
Space group	$P2_12_12_1$	P1	$P2_1$
a [Å]	6.62420(10)	10.8847(4)	10.1338(5)
b [Å]	9.0132(2)	12.2073(4)	6.9394(3)
c [Å]	27.3581(5)	13.9766(4)	12.6999(6)
α [°]	90	75.205(2)	90
β [°]	90	73.759(2)	98.797(2)
γ [°]	90	85.9442(17)	90
V [Å^3]	1633.42(5)	1723.89(10)	882.58(7)
Z	4	4	2
ρ_{calcd} [g cm^{-3}]	1.70296(5)	1.631	1.64365(13)
μ [mm^{-1}]	1.171	1.112	1.091
Absorption correction	Numerical	Multi-scan	Numerical
T_{min}, T_{max}	0.8404, 0.8717	0.917, 0.975	0.8313, 0.9765
Refls. measured	27,634	11,792	9457
R_{int}	0.0920	0.039	0.0807
Mean σ(*I*)/*I*	0.0595	0.0376	0.0730
θ range	3.18–27.49	3.18–25.40	3.25–25.16
Observed refls.	3185	11,256	2785
x, *y* (weighting scheme)	0.0435, 1.7950	0.0313, 1.4978	0.0189, 0
Flack parameter	−0.04(5)	−0.032(17)	−0.08(5)
Refls. in refinement	3755	11,792	3118
Parameters	205	864	230
Restraints	3	30	7
$R(F_{obs})$	0.0434	0.0301	0.0358
$R_w(F^2)$	0.0946	0.0725	0.0792
S	1.030	1.077	1.049
Shift/error$_{max}$	0.001	0.001	0.001
Max. res. density [eÅ^{-3}]	1.547	0.706	0.662
Min. res. density [eÅ^{-3}]	−0.616	−0.829	−0.535

Table 8
Crystallographic data for **4**–**5**

	4	**5**
Empirical formula	$C_{24}H_{58}N_4O_{15}Pd_2$	$C_{12}H_{28}N_2O_6Pd$
M_r [g mol^{-1}]	855.58	402.78
Crystal size [mm]	0.25 × 0.18 × 0.02	0.27 × 0.16 × 0.14
Crystal system	Monoclinic	Monoclinic
Space group	C2	$P2_1$
a [Å]	18.9330(5)	8.8758(3)
b [Å]	6.8860(2)	18.5971(6)
c [Å]	14.4389(4)	10.3814(4)
α [°]	90	90
β [°]	115.3663(15)	106.680(4)
γ [°]	90	90
V [Å^3]	1700.95(8)	1641.50(10)
Z	2	4
ρ_{calcd} [g cm^{-3}]	1.67052(8)	1.62983(10)
μ [mm^{-1}]	1.129	1.157
Absorption correction	Numerical	Numerical
T_{min}, T_{max}	0.7756, 0.9749	0.8312, 0.8806
Refls. measured	13,959	16,208
R_{int}	0.0406	0.0308
Mean $\sigma(I)/I$	0.0406	0.0614
θ range	3.19–27.51	3.73–27.53
Observed refls.	3426	6039
x, y (weighting scheme)	0.0203, 1.7244	0.0175, 0
Flack parameter	−0.04(3)	−0.034(18)
Refls. in refinement	3745	7304
Parameters	223	403
Restraints	8	7
$R(F_{obs})$	0.0271	0.0291
$R_w(F^2)$	0.0597	0.0466
S	1.053	0.897
Shift/error$_{max}$	0.001	0.001
Max. res. density [eÅ^{-3}]	0.873	0.678
Min. res. density [eÅ^{-3}]	−0.668	−0.432

24 h at 4 °C. Cold water (0.4 mL) and cold acetone (6.0 mL) were added to 1 mL of the solution. Subsequently, acetone vapours were allowed to diffuse into the solution. Yellow crystals were formed within 3 weeks at 5 °C.

4.4.4. (1*R*,2*R*)-Cyclohexane-1,2-diamine(methyl β-D-xylopyranos-2,3-*O*-diato)palladium(II) 2.5-hydrate

Methyl β-D-xylopyranoside (164.0 mg, 1.0 mmol) was dissolved in [Pd(*R*,*R*-chxn)(OH)$_2$] (5 mL, 0.3 M, 0.45 mmol), and stirred for 24 h at 4 °C. Cold water (0.6 mL) and cold acetone (1.5 mL) were added to 1 mL of the solution. Subsequently, acetone vapours were allowed to diffuse into the solution. Yellow crystals were formed within 3 weeks at 5 °C.

4.4.5. *N*,*N*,*N*′,*N*′-Tetramethylethane-1,2-diamine(methyl β-D-xylopyranosdiato)palladium(II) cocrystallisate

Methyl β-D-xylopyranoside (44.0 mg, 0.225 mmol) was dissolved in [Pd(tmen)(OH)$_2$] (1 mL, 0.45 M, 0.45 mmol), and stirred for 2 h at 4 °C. The solution was saturated with acetone. Subsequently, acetone vapours were allowed to diffuse into the solution. Pale yellow crystals were formed within 4 month at 5 °C.

4.5. Crystal structure determination and refinement

Crystals suitable for X-ray crystallography were selected with the aid of a polarisation microscope, mounted on the tip of a glass fibre and investigated at 200 K on a Nonius KappaCCD diffractometer with graphite-monochromated MoK radiation (λ = 0.71073 Å). Numerical absorption correction (SCALEPACK) was applied. The structures were solved by direct methods (SIR97) and refined by full-matrix, least-squares calculations on F^2 (SHELXL-97). Anisotropic displacement parameters were refined for all non-hydrogen atoms.[33,34] The refined structures were analysed with PLATON including a puckering analysis, and visualised with ORTEP; the puckering parameter φ is given for θ >5° only.[27,35,36] Crystallographic data are listed in Table 7 and 8.

Acknowledgement

This work has been funded by the Deutsche Forschungsgemeinschaft (Grant Kl 624/12-1).

Supplementary data

CCDC 781712 (**1**), 781713 (**2**), 781714 (**3**), 781715 (**4**), and 781716 (**5**) contain the supplementary crystallographic data for this paper. These data can be obtained free of charge from the Cambridge Crystallographic Data Center via www.ccdc.cam.ac.uk/data_request/cif. Supplementary data associated with this article can be found, in the online version, at doi:10.1016/j.carres.2010.08.006.

References

1. Schwarz, T.; Heß, D.; Klüfers, P. *Dalton Trans.* **2010**, *39*, 5544–5555.
2. Ghaschghaie, N.; Hoffmann, T.; Steinborn, M.; Klüfers, P. *Dalton Trans.* **2010**, *39*, 5535–5543.
3. Gilg, K.; Mayer, T.; Ghaschghaie, N.; Klüfers, P. *Dalton Trans.* **2009**, 7934–7945.
4. Arendt, Y.; Labisch, O.; Klüfers, P. *Carbohydr. Res.* **2009**, *344*, 1213–1224.
5. Klüfers, P.; Kopp, F.; Vogt, M. *Chem. Eur. J.* **2004**, *10*, 4538–4545.
6. Klüfers, P.; Kunte, T. *Chem. Eur. J.* **2003**, *9*, 2013–2018.
7. Klüfers, P.; Kunte, T. *Eur. J. Inorg. Chem.* **2002**, *2002*, 1285–1289.
8. Klüfers, P.; Kunte, T. *Angew. Chem., Int. Ed.* **2001**, *40*, 4210–4212.
9. Reeves, R. E. *Adv. Carbohydr. Chem.* **1951**, *6*, 107–134.
10. Rao, V. S. R.; Qasba, P. K.; Balaji, P. V.; Chandrasekaran, R. *Conformation of Carbohydrates*; Harwood Academic: Amsterdam, 1998.
11. Schweizer, E. *J. Prakt. Chem.* **1857**, *72*, 109–111.
12. Kettenbach, G.; Klüfers, P.; Mayer, P. *Macromol. Symp.* **1997**, *120*, 291–301.
13. Burchard, W.; Habermann, N.; Klüfers, P.; Seger, B.; Wilhelm, U. *Angew. Chem., Int. Ed. Engl.* **1994**, *33*, 884–887.
14. Traube, W. *Ber. Dtsch. Chem. Ges.* **1911**, *44*, 3319–3324.
15. Jayme, G.; Neuschäffer, K. *Naturwissenschaften* **1957**, *44*, 62–63.
16. Jayme, G.; Neuschäffer, K. *Die Makromol. Chem.* **1957**, *23*, 71–83.
17. Reeves, R. E. *J. Am. Chem. Soc.* **1949**, *71*, 215–217.
18. Reeves, R. E. *J. Am. Chem. Soc.* **1949**, *71*, 212–214.
19. Reeves, R. E. *J. Am. Chem. Soc.* **1950**, *72*, 1499–1506.
20. Reeves, R. E.; Bragg, P. *J. Org. Chem.* **1961**, *26*, 3487–3489.
21. Ahlrichs, R.; Ballauff, M.; Eichkorn, K.; Hanemann, O.; Kettenbach, G.; Klüfers, P. *Chem. Eur. J.* **1998**, *4*, 835–844.
22. Kästele, X.; Klüfers, P.; Kunte, T. Z. *Anorg. Allg. Chem.* **2001**, *627*, 2042–2044.
23. Allscher, T.; Klüfers, P.; Labisch, O. *Carbohydr. Res.* **2007**, *342*, 1419–1426.
24. Allscher, T.; Kästele, X.; Kettenbach, G.; Klüfers, P.; Kunte, T. *Chem. Asian J.* **2007**, *2*, 1037–1045.
25. Dowd, M.; Rockey, W.; French, A.; Reilly, P. *J. Carbohydr. Chem.* **2002**, *21*, 11.
26. Bock, K.; Thøgersen, H.. In *Annual Reports on NMR Spectroscopy*; Webb, G. A., Ed.; Academic Press, 1983; Vol. 13, pp 1–57.
27. Cremer, D.; Pople, J. A. *J. Am. Chem. Soc.* **1975**, *97*, 1354–1358.
28. Connelly, N. G.; Damhus, T.; Hartshorn, R. M.; Hutton, A. T. *Nomenclature of Inorganic Chemistry: IUPAC Recommendations 2005*; The Royal Society of Chemistry: Cambridge, 2005.
29. Cortes-Guzman, F.; Hernandez-Trujillo, J.; Cuevas, G. *J. Phys. Chem. A* **2003**, *107*, 9253–9256.
30. Ribeiro, D. S.; Rittner, R. *J. Mol. Struct.* **2003**, *657*, 85–92.
31. Kim, J.-Y. *Arch. Pharm. Res.* **1992**, *15*, 336–342.
32. Haasnoot, C. A. G.; de Leeuw, F. A. A. M.; Altona, C. *Tetrahedron* **1980**, *36*, 2783–2792.
33. Altomare, A.; Burla, M. C.; Camalli, M.; Cascarano, G. L.; Giacovazzo, C.; Guagliardi, A.; Moliterni, A. G. G.; Polidori, G.; Spagna, R. *J. Appl. Crystallogr.* **1999**, *32*, 115–119.
34. Sheldrick, G. *Acta Crystallogr., Sect. A* **2008**, *64*, 112–122.
35. Spek, A. *J. Appl. Crystallogr.* **2003**, *36*, 7–13.
36. Farrugia, L. *J. Appl. Crystallogr.* **1997**, *30*, 565.